# Molecular and Functional Differences between Heart mKv1.7 Channel Isoforms

Rocio K. Finol-Urdaneta,[1,2] Nina Strüver,[1,3] and Heinrich Terlau[1,4]

[1]Max-Planck-Institute for Experimental Medicine, Group of Molecular and Cellular Neuropharmacology, 37075 Göttingen, Germany
[2]Department of Physiology and Biophysics, University of Calgary, Calgary T2N4N1, Canada
[3]Medizinische Hochschule Hannover, Abteilung Gastroenterologie, Hepatologie, und Endokrinologie, 30623 Hannover, Germany
[4]Institute for Experimental and Clinical Pharmacology and Toxicology, Universitätsklinikum Schleswig-Holstein, 23538 Lübeck, Germany

Ion channels are membrane-spanning proteins that allow ions to permeate at high rates. The kinetic characteristics of the channels present in a cell determine the cell signaling profile and therefore cell function in many different physiological processes. We found that Kv1.7 channels from mouse heart muscle have two putative translation initiation start sites that generate two channel isoforms with different functional characteristics, mKv1.7L (489 aa) and a shorter mKv1.7S (457 aa). The electrophysiological analysis of mKv1.7L and mKv1.7S channels revealed that the two channel isoforms have different inactivation kinetics. The channel resulting from the longer protein (L) inactivates faster than the shorter channels (S). Our data supports the hypothesis that mKv1.7L channels inactivate predominantly due to an N-type related mechanism, which is impaired in the mKv1.7S form. Furthermore, only the longer version mKv1.7L is regulated by the cell redox state, whereas the shorter form mKv1.7S is not. Thus, expression starting at each translation initiation site results in significant functional divergence. Our data suggest that the redox modulation of mKv1.7L may occur through a site in the cytoplasmic N-terminal domain that seems to encompass a metal coordination motif resembling those found in many redox-sensitive proteins. The mRNA expression profile and redox modulation of mKv1.7 kinetics identify these channels as molecular entities of potential importance in cellular redox-stress states such as hypoxia.

The Journal of General Physiology

## INTRODUCTION

Ion channels are specialized membrane-spanning proteins through which ions permeate at a high rate during the open conformation of the pore. Voltage-gated $K^+$ (Kv) channels are indispensable for the electrical excitability of nerve and muscle fibers because they are responsible for cell membrane repolarization after initiation of an action potential. Voltage-gated $K^+$ channels are known to modulate synaptic transmission and secretion from endocrine cells, such as insulin from pancreatic islet cells (MacDonald et al. 2001). The basic electrophysiological characteristics (i.e., kinetics) of Kv channels contribute importantly to the modulation of the shape, frequency, and duration of the cardiac action potential (Nerbonne, 2000; Brown, 2004).

The N-terminal region of the Kv channels plays important regulatory roles, including inactivation kinetics (Bezanilla and Armstrong, 1977; Hoshi et al., 1990; Zagotta et al., 1990; MacKinnon et al., 1993; Roeper et al., 1998; Pongs et al., 1999), subunit recognition (Li et al., 1992; Shen and Pfaffinger, 1995), and redox modulation of the currents flowing through those channels (Ruppersberg et al., 1991; Ciorba et al. 1997, 1999). Thus, the differences among N-terminal regions of Kv channels can result in important functional differences between the different molecular forms of Kv channels.

Correspondence to Heinrich Terlau: hterlau@gwdg.de

Kv1.7 channels are the most recently cloned members of the Kv1 family of voltage-activated potassium channels. From previous work it is known that the murine Kv1.7 channels are encoded by the *Kcna7* gene, composed of two exons separated by a 1.9-kb intron, and it is located in the mouse chromosome 7 (Kalman et al., 1998). Transcripts of the *Kcna7* gene are reported present in several tissues, including strong expression in the heart and skeletal muscle. Furthermore, *Kcna7* transcripts have been found in the mouse mesenteric artery (Fountain et al., 2004), as well as in the rat main and small pulmonary arteries (Davies and Kozlowski, 2001). However, the literature about the biophysical and pharmacological characteristics of the murine Kv1.7 channels is scarce and controversial.

Here we report the cloning and functional expression of Kv1.7 channels from the mouse heart muscle (mKv1.7). Previously, mKv1.7 current characteristics were described with very fast inactivation (Kalman et al., 1998), as well as slow inactivation (Bardien-Kruger et al., 2002). The presence within the same open reading frame (ORF) of two putative translation initiation codons (AUG) suggested a means to generate functionally

Abbreviations used in this paper: DTDP, dithiodipyridine; DTT, dithiotreithol; NFR, normal frog Ringer; TEVC, two electrode voltage clamp.

different channels from translation initiation at each site. Therefore, we have performed a detailed electrophysiological characterization of mKv1.7L channels and the predicted shorter translation product mKv1.7S, which lacks the N-terminal region between the two translation initiation start sites (32 aa).

Taking into account the discrepancies in the cDNA sequences of *Kcna7* as reported previously, this work represents the first electrophysiological characterization of the Kv1.7 channel from the mouse heart; and provides an alternative explanation for the differences observed in former descriptions of mKv1.7 channels. Moreover, we have found that mKv1.7L channels are redox sensitive, and we were able to identify molecular determinants of the different channel kinetics and redox sensitivity of mKv1.7 channels through a combined molecular/electrophysiological analysis.

## MATERIALS AND METHODS

Cloning procedures were performed according to standard methods (Sambrook et al., 1989). All cloning strategies, including sequence analysis, primer design, restriction mapping, and sequence alignments, were assisted by the Lasergene software (DNAstar).

Total RNA from adult mouse heart and skeletal muscle were isolated with RNAeasy mini kit (QIAGEN) and TRIzol LS Reagent (Invitrogen). Self-prepared RNA and BD Premium Total mouse heart RNA (CLONTECH Laboratories, Inc.) were used as templates for RT-PCR cDNA synthesis. Primers were designed after the *Kcna7* sequence from the GenBank/EMBL/DDBJ (accession no. AF032099).

The 5′ fragment was a 670-bp cDNA fragment corresponding to the 5′ end of the *Kcna7* gene amplified using one step RT-PCR (Advantage RT-PCR kit; Invitrogen) with primers 5′-GCC ACA CGT CCG TTC ACC GGT C-3′ and 5′-AGA ATG GAT CGT TGA AGG GCT GTC-3′ according to the manufacturer's protocol; 2 mM $MgSO_4$ and 10% DMSO were added. Conditions were as follows: first strand synthesis, 30 min at 60°C; hot start, 2 min at 94°C; 40 cycles of denaturation (15 s at 94°C), annealing (30 s, 67°C), and extension (45 s, 68°C). The final extension was 5 min at 68°C.

The 3′ fragment was the 3′ end of the *Kcna7* gene amplified by "gene-specific primer" reverse transcription (GSP-RT), followed by PCR. GSP-RT was performed with Superscript II (Invitrogen) with antisense primer 5′-CCC TAG GAA TCT GTA CCC GCA CCA TG-3′. Platinum *Pfx* DNA Polymerase (Invitrogen) was used for nested PCR.

The first round primers were 5′-TCT GGC TGC TCT TCG AAT TTC CTG AGA-3′ and 5′-CCC TAG GAA TCT GTA CCC GCC ACC ATG-3′. Cycling conditions were as follows: hot start, 2 min at 94°C; 30 cycles of denaturation (15 s at 94°C), annealing (30 s, 58°C), and extension (1.5 min, 68°C). The final extension was 5 min at 68°C. The second round PCR primers were 5′-TCC GAA TTC GTC ATC CTG GTC TCC A-3′ and antisense 5′-ATT GGG CCC TCA CAC CTC AGT CAC CAT GTG-3′. Cycling conditions were as follows: hot start, 2 min at 94°C; 30 cycles of denaturation (15 s at 94°C), annealing (30 s, 55°C), and extension (1 min, 68°C). The final extension was 5 min at 68°C.

All constructs were subcloned into pGem T-easy vector (Promega) and sequenced on an Applied Biosystems 373 DNA sequencer (Applied Biosystems). cDNA constructs were subcloned in the modified pSGEM expression vector (Liman et al., 1992) and transcribed in vitro with the T7 Polymerase (Stratagene), rendering capped cRNAs.

### Functional Analysis of mKv1.7 Channels

The *Xenopus laevis* oocyte heterologous expression system was used for functional analysis of mouse Kv1.7 subunits. Oocytes were surgically removed from anesthetized female *Xenopus laevis* (20–30 min in 1.25 g/liter tricaine) and defolliculated by partial enzymatic digestion with Collagenase type 2 (440 U/ml, Worthington Biochemical Corporation). The wash and storage solution was Barth medium: (in mM) 88 NaCl, 1 KCl, 7.5 Tris-HCl, 2.4 $NaHCO_3$, 0.82 $MgSO_4$, 0.33 $Ca(NO_3)_2$, 0.41 $CaCl_2$; 230–240 mosm, pH 7.4 (NaOH adjusted). Oocytes from stages IV–VI were microinjected with 50 nl of cRNA and incubated at 17°C in antibiotic supplemented Barth medium (24–72 h) before electrophysiological analysis.

### Electrophysiology

Two electrode voltage clamp (TEVC) recordings were performed using a Turbo TEC-10 (npi electronics) with electronic built-in series resistance compensation. The electrical stimulation and registration of the current was performed through the EPC9 built-in ITC-16 AD/DA converter, controlled by a Macintosh G4 computer (Apple). Data acquisition was made using Pulse software (HEKA). An electronic series resistance (Rs) measurement device was used in conjunction with a standard TEVC amplifier to follow and display the Rs automatically (Polder et al., 2003). TEVC microelectrodes were made from borosilicate filament glass capillaries (Hilgenberg) and filled with 2 M KCl. Patch clamp pipettes were made from borosilicate Kimax-51 glass capillaries (Kimble) and had resistance between 1 and 4 MΩ. The patch pipette filling solution contained 115 mM KCl, 1.8 mM EGTA, and 10 mM HEPES. Currents measured during TEVC and patch experiments were subtracted online with a standard P/4 protocol (Armstrong and Bezanilla, 1973). Current signals were sampled at 250–100 μs (sampling rate: 4–10 kHz) for TEVC, and at 50 μs (sampling rate: 20 kHz) for patch recordings. Signals were low pass filtered with a Bessel filter at 1–2.5 kHz for TEVC and 5 kHz for patch clamp recordings. The standard extracellular bath recording solution was normal frog Ringer (NFR) containing (in mM) 115 NaCl, 2.5 KCl, 1.8 $CaCl_2$, 10 HEPES-NaOH; pH7.2. All experiments were performed at room temperature (20–22°C).

Data acquisition was performed with Pulse/PulseFit software package (HEKA). Off-line analysis was performed with a Macintosh G4 microcomputer (Apple) with Igor Pro (Wavemetrics, Inc). All data is expressed as mean ± SEM. Two tailed t-tests were used to evaluate the significance of the difference between means ($P < 0.05$).

Macroscopic conductance was calculated according to $G_K = I_K(E_m - E_K)$, where $G_K$ is the total potassium conductance, $I_K$ is the total current, $E_m$ is the command potential, and $E_K$ corresponds to the experimentally obtained average potassium equilibrium potential (−97 mV; not depicted). G values were normalized to maximal conductance ($G_K/G_{max}$).

Boltzmann fits were calculated according to $G/G_{max} = \text{Offset} + 1/(1 + \exp^{((V1/2 - Vm)/a)})$, where $V_{1/2}$ is the half activation or inactivation potential and *a* is the slope parameter.

## RESULTS

We cloned *Kcna7* cDNA that encodes Kv1.7 channels from mouse heart and skeletal muscle. The first AUG codon generated a Kv1.7 protein of 489 amino acids (mKv1.7L), and downstream of it, a second AUG within an ideal Kozak consensus sequence was found (Kozak, 1991) that originates a shorter protein mKv1.7S (457 aa) (Fig. 1 A). mKv1.7S lacks the most N-terminal 32 aa

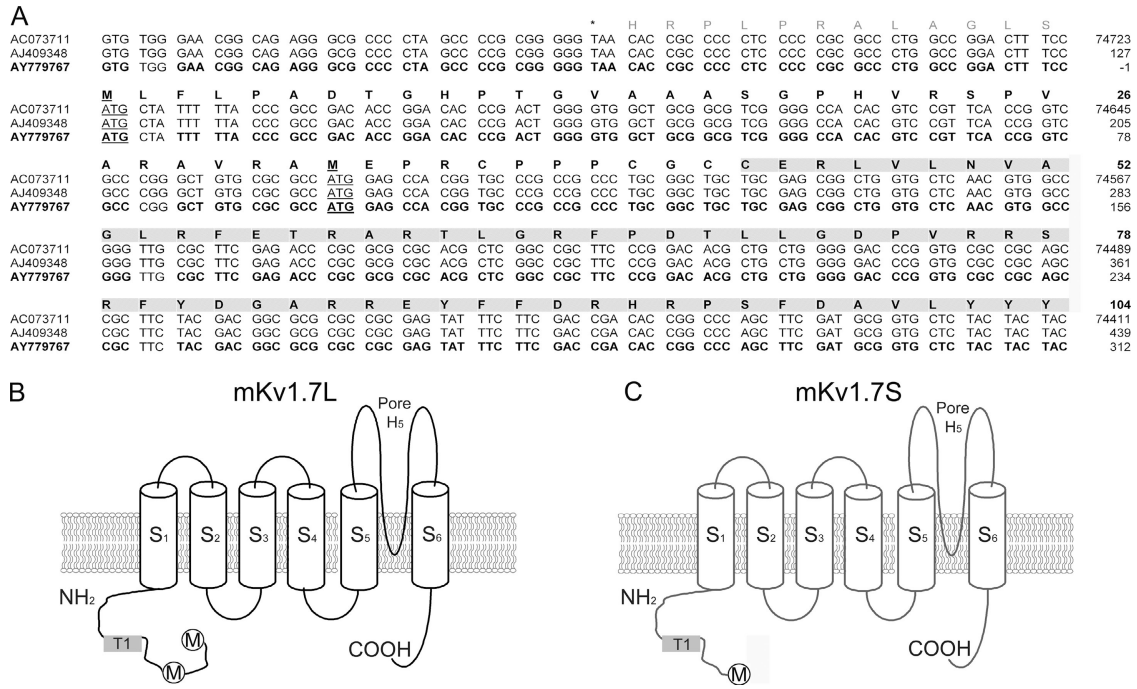


**Figure 1.** mKv1.7 nucleotide and amino acid sequence. (A) Sequence alignment of the 5′ region of *Kcna7*. Nucleotide and amino acid sequence corresponding to the 5′ UTR and coding sequence for the cytoplasmic N-terminal domain of the mKv1.7 channels. The mouse chromosome 7 sequence AC073711, mouse cDNA fragment AJ409348 (Kashuba et al., 2001), and accession no. AY779767 (this work) sequences are >99% identical. Stop codon is marked with an asterisk, and initiation of the translation sites are underlined. Amino acids in bold correspond to the putative mKv1.7 N-terminal domain. (B and C) Schematic representation of the mKv1.7L and mKv1.7S constructs including the six hydrophobic domains (S1–S6), N and C cytoplasmic termini, and the pore region (H5). Initiation methionines are indicated by circles. The T1 domain is indicated by gray shaded boxes.

that are located between the aforementioned AUGs (Fig. 1, A and C). Fig. 1 A shows the sequence of the cDNA 5′ end and the cytoplasmic N-terminal domain of the predicted protein of mouse Kv1.7 channels. Both initiation codons are underlined in the alignment of our sequence (GenBank/EMBL/DDBJ accession no. AY779767), with the mouse chromosome 7 genomic sequence (accession no. AC073711), and a partial cDNA (accession no. AJ409348) cloned by Kashuba et al. (2001) (Fig. 1 A). Curiously, previous reports failed to identify the first ATG as a functional initiation of the translation site for *Kcna7* transcripts (Kalman et al., 1997; Kashuba et al., 2001; Bardien-Kruger et al., 2002). Fig. 1 (B and C) contains schematic representations of the channels formed by Kv1.7L and Kv1.7S proteins showing the N and C termini that reside in the intracellular side of the membrane, six hydrophobic segments (S1–S6), and a well-defined pore region that has the potassium-selective signature sequence "TVGYG." Both channels were expressed heterologously in *Xenopus laevis* oocytes and were fully functional during TEVC and patch clamp experiments (Fig. 2).

### Characteristics of mKv1.7L and mKv1.7S Channels

Evoked currents from mKv1.7L and mKv1.7S channels in response to standard I/V protocols from TEVC recordings are shown in A and B of Fig. 2. Outward currents were elicited by 500 ms depolarizing pulses from −60 to +80 mV (holding potential, $V_h$ = −100 mV) with NFR as the extracellular solution. As can be directly seen, the main difference in the channel current characteristics is that the inactivation kinetics of mKv1.7L is faster than that of mKv1.7S. The electrophysiological analysis of the steady-state activation process is shown in Fig. 2 C and Table I. mKv1.7L and Kv1.7S start to activate at potentials more positive than −30 mV. Relative conductance versus potential plots were accurately fit by a Boltzmann equation (Fig. 2 C) with similar slopes of the steady-state activation curves for the evoked currents (mKv1.7L, 15.4 ± 05 mV; mKv1.7S, 13.3 ± 0.6 mV). Nevertheless, the absence of 32 amino acids in the N-terminal region of mKv1.7S apparently caused a small but statistically significant shift in the voltage of activation, resulting in an ∼8-mV difference in half activation potential ($V_{1/2}$: mKv1.7L, 4.4 ± 1.4 mV; mKv1.7S, −4.3 ± 2.9 mV; $P < 0.01$). The former suggests some influence of the N-terminal region on voltage sensing in mKv1.7 channels.

Not only was the steady-state activation of mKv1.7 channels affected by the N-terminal 32 amino acids, but the activation kinetics was influenced as well. The activation of mKv1.7 currents was assessed in a model-independent

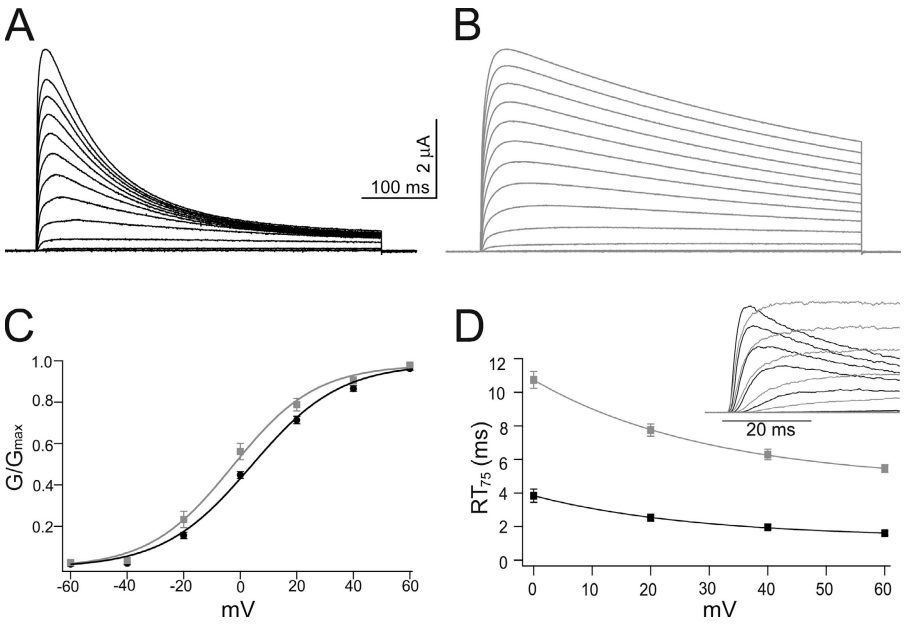


**Figure 2.** Activation of mKv1.7 channels. Representative outward currents in response to 500-ms depolarizing test potentials ranging from −60 to +80 mV in 10-mV increments, extracellular solution NFR, $V_h$ = −100 mV. mKv1.7L is shown in black (A) and mKv1.7S in gray (B). (C) Steady-state activation curves for mKv1.7L ($n$ = 20, black) and mKv1.7S ($n$ = 15, gray). Mean ± SEM of the relative conductances are plotted against the potential. The smooth line corresponds to Boltzmann fits to the data. (D) Rise time plot of mKv1.7L ($n$ = 13) and mKv1.7S ($n$ = 20) currents measured as the time in ms required for reaching 75% of $I_{max}$ ($RT_{75}$) from on-cell patch clamp experiments. mKv1.7L data are shown in black and mKv1.7S in gray. The inset in D presents superimposed early current traces of on-cell patch clamp recordings of mKv1.7L and mKv1.7S channels.

manner by determining the time required to reach 75% of the peak outward current ($RT_{75}$) at different potentials. The inset in Fig. 2 D presents superimposed traces of on-cell patch clamp recordings of mKv1.7L and mKv1.7S channels corresponding to the initial times of envelopes of currents elicited by progressive depolarizations. The $RT_{75}$ values from on-cell patch clamp experiments are plotted against the potential in Fig. 2 D, showing that mKv1.7L currents reach the peak amplitude approximately three times faster than the mKv1.7S currents at all voltages examined. $RT_{75}$ for mKv1.7L was ∼2 ms at +40 mV, while mKv1.7S currents reached 75% of the peak amplitude within 6 ms ($P = 0.0001$). There were no significant differences between TEVC (Table I) and the corresponding patch datasets for the channels studied.

### Inactivation of mKv1.7 Channels

Protein sequences of mKv1.7L and Kv1.7S channels are identical except for the first 32 amino acids at the N terminus predicted to reside in the cytoplasmic side of the membrane. It has been thoroughly reported that partial deletion of the N-terminal region of Kv channels alters N-type inactivation (Hoshi et al., 1990; Furukawa, 1995; Lee et al., 1996). Therefore the differences in the inactivation kinetics between mKv1.7L and Kv1.7S channels were suspected to be related to N-type inactivation process. Fig. 3 A shows overlaid TEVC current traces in response to 2.5-s depolarization of the mouse Kv1.7L and Kv1.7S channels. The mKv1.7L channels inactivated rapidly and almost completely at +40 mV (∼5% steady-state current left); whereas mKv1.7S currents exhibited 27% residual current after 2.5 s (Fig. 3 B). Inactivation data in response to 2.5-s stimulations were fit to an exponential decay; mKv1.7L currents could be satisfactorily fit to a single exponential function between 50 and 500 ms of the pulse, and mKv1.7S between 50 and 2,500 ms. The time constants derived ($\tau_{Inac}$) were monotonically and weakly voltage dependent as expected for N-type inactivation (Fig. 3 C). Statistical analysis of the inactivation time constant ($\tau_{Inac}$) of mKv1.7L currents over all the potentials evaluated showed them to be

TABLE I

*Characteristics of the Currents Mediated by mKv1.7L and mKv1.7S Channels Expressed in Xenopus Oocytes Determined by TEVC Measurements*

| | $V_{1/2}$ | Slope | $RT_{75}$ | $\tau_{Inac}$ | $V_{1/2}$Inac | $Slope_{Inac}$ | $\tau_{Rec1}$ | $\tau_{Rec2}$ | $\tau_{CI}$ 2.5 mM $K^+$ | $\tau_{CI}$ 117.5 mM $K^+$ |
|---|---|---|---|---|---|---|---|---|---|---|
| | *mV* | | *ms* | *ms* | *mV* | *mV* | *ms* | *s* | *s* | *s* |
| mKv1.7L | 4.4 ± 1.4 | 15.4 ± 0.5 | 4.4 ± 0.5 | 181.8 ± 15.4 | −40 ± 0.7 mV | 4 ± 0.3 | 1.2 ± 0.1 | 45.3 ± 4.5 | 8.1 ± 0.3 | 22.5 ± 4.4 |
| | $n$ = 20 | $n$ = 20 | $n$ = 12 | $n$ = 15 | n = 5 | $n$ = 5 | $n$ = 15 | $n$ = 15 | $n$ = 20 | $n$ = 23 |
| mKv1.7S | −4.3 ± 2.9 | 13.3 ± 0.6 | 7.5 ± 0.7 | 643.2 ± 80.1 | −21 ± 2 mV | 7 ± 0.7 | 0.8 ± 0.1 | 34.6 ± 1.9 | 14.1 ± 4.8 | 38 ± 14.6 |
| | $n$ = 15 | $n$ = 15 | $n$ = 12 | $n$ = 13 | $n$ = 5 | $n$ = 5 | $n$ = 9 | $n$ = 9 | $n$ = 6 | $n$ = 5 |
| | ** | ns | ** | *** | *** | ** | ** | ns | ** | ** |

$RT_{75}$ and $\tau_{Inac}$ are at + 40 mV. $\tau_{Rec1}$ and $\tau_{Rec2}$ are the time constants for the recovery from inactivation. ns, not significant. *, $P < 0.01$; **, $P < 0.001$; ***, $P = 0.0001$.

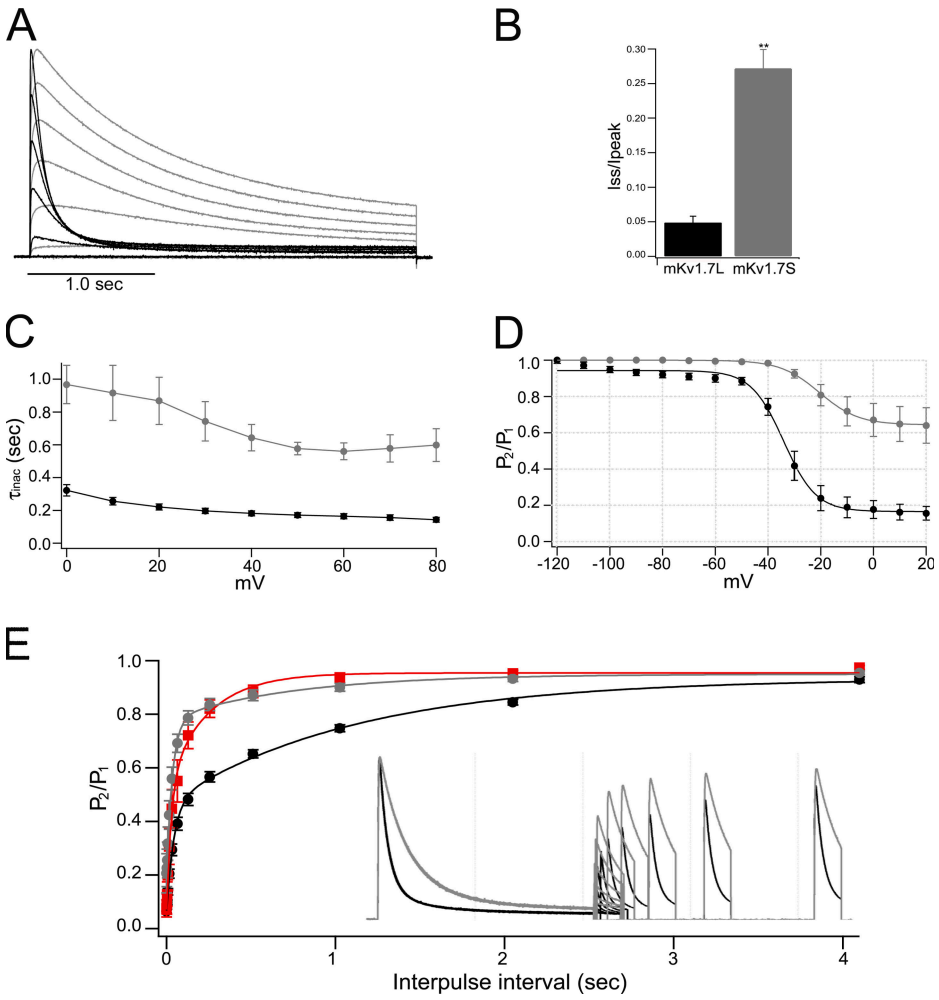


**Figure 3.** Inactivation of mKv1.7 channels. (A) Normalized and superimposed mKv1.7L (black) and mKv1.7S (gray) TEVC current traces elicited by a 2.5-s pulse from −60 to +80 mV, in 20-mV steps. (B) Bar diagram of the fractional current (steady-state current divided by peak current amplitude, $I_{ss}/I_{peak}$) of Kv1.7L and Kv1.7S channels ($n$ = 15 and $n$ = 13, respectively). (C) Inactivation time constants derived from monoexponential fits to the inactivation process, mKv1.7L ($n$ = 15) and mKv1.7S ($n$ = 13). (D) Steady-state inactivation was estimated by measuring the peak current amplitude elicited by 30-ms test pulses to 40 mV after 1.5-s prepulses to a −120 to 20 mV potential range. Current is plotted as a fraction of the maximum peak current and fitted with a Boltzmann function ($n$ = 6 and 5 for mKv1.7L and mKv1.7S, respectively). (E) Recovery from inactivation. Time course of the recovery from inactivation of mKv1.7L and Kv1.7S channels is shown in the inset. The mean ± SEM $P_2/P_1$ ratio is shown as a function of time ($2.5K^+_o$ mKv1.7L: black, $n$ = 15; $2.5K^+_o$ mKv1.7S: gray, $n$ = 6; 117.5 $K^+_o$ mKv1.7L: red, $n$ = 4).

significantly faster than those obtained from mKv1.7S currents (TEVC at +40 mV, $L\tau_{Inac}$ 182 ± 16 ms, and $S\tau_{Inac}$ 643 ± 80 ms, $P < 0.001$) (Table I). Thus, steady-state inactivation of mKv1.7L channels is significantly different from that of mKv1.7S, as shown in Fig. 3 D and Table I. The average midpoint potential for steady-state inactivation of mKv1.7L channels was −40 ± 0.7 mV with a slope parameter of 4 ± 0.3 mV, where after 1.5 s of interpulse interval, ∼15% of the current did not inactivate further.

Inactivation of Kv1.7S channels was less complete, less voltage dependent, and had a more depolarized $V_{1/2}$ for the onset of inactivation (∼65% noninactivating after 1.5-s interpulse interval, 7 ± 0.7 mV slope, and steady-state inactivation $V_{1/2}$ = −21 ± 2 mV). Neither $V_{1/2}$ nor voltage dependence were altered by raising the extracellular potassium concentration to 50 mM for Kv1.7L or Kv1.7S channels at interpulse intervals between 250 ms and 1.5 s (unpublished data).

Recovery from inactivation was faster in mKv1.7S channels. The inactivation recovery protocol consisted of two depolarizing pulses to +40 mV spaced by increasingly long interpulse intervals at −100 mV. Scaled and superimposed current traces from mKv1.7L and mKv1.7S are shown in the inset of Fig. 3 E. The recovery from inactivation revealed two time constants ($\tau_{Rec1}$ and $\tau_{Rec2}$), suggesting the presence of two inactivation processes kinetically different but mutually coupled. In agreement to the observed inactivation features of both channels, the recovery resulted faster for the slow inactivating mKv1.7S than for the faster inactivating mKv1.7L channel (mKv1.7S$\tau_{Rec1}$ 0.8 ± 0.1 s vs. mKv1.7L$\tau_{Rec1}$ 1.2 ± 0.1 s, $P = 0.002$). In support of an N-type–related inactivation process in mKv1.7L, the recovery from inactivation is significantly faster in the presence of high $[K^+]_o$ only for the Kv1.7L channels (mKv1.7L $K^+\tau_{Rec1}$ 0.7 ± 0.3 s, Fig. 3 E).

Previous reports suggest that mKv1.7 channels can accumulate in the inactivated state. The time course of cumulative inactivation, a rapid decline in the peak current amplitude elicited by successive depolarizing test pulses, from mKv1.7L and Kv1.7S channels, is shown in Fig. 4. Current amplitude decreased during 5-s-long stimulations to +40 mV every 1 s ($V_h$ = −100 mV; Fig. 4 C, inset). Pulses were long enough to achieve a comparable level of inactivation from fast and slow inactivating

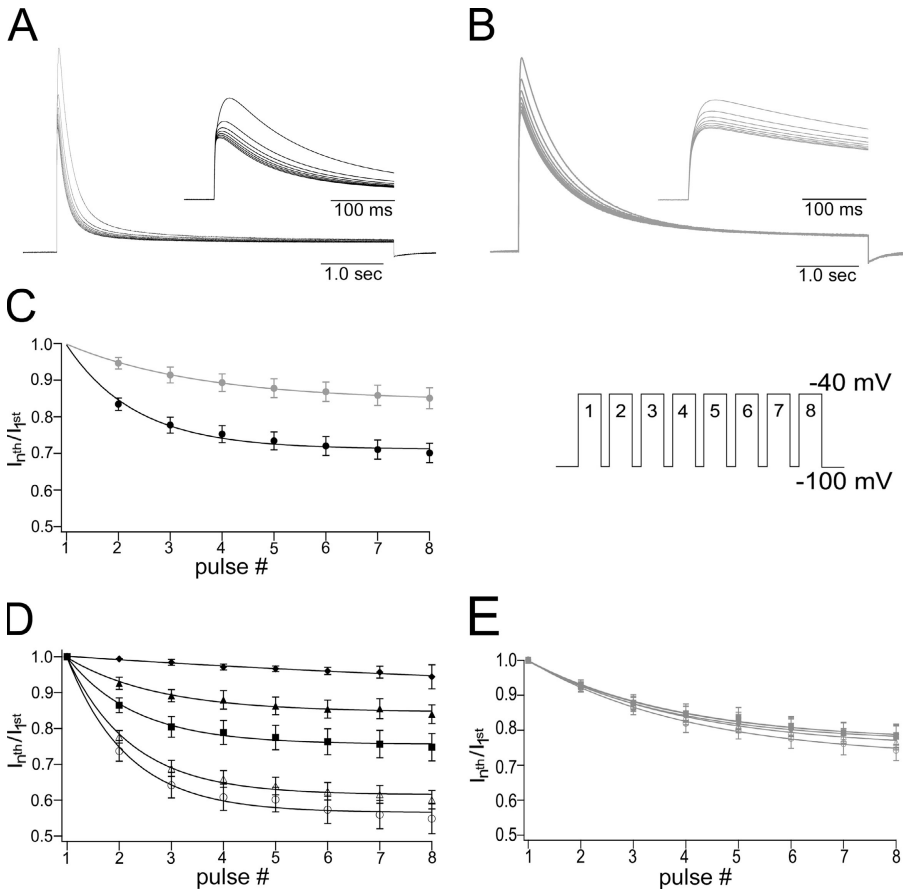


**Figure 4.** Cumulative inactivation of mKv1.7 channels, $[K^+]_o$ dependence. Currents were elicited by a train of depolarizing pulses with duration of 5 s to +40 mV with an interpulse interval of 1 s from a $V_h$ of −100 mV (inset in C). (A and B) Eight consecutive current traces from mKv1.7L and mKv1.7S, respectively. The insets contain first 500 ms of the corresponding currents of mKv1.7L in black and mKv1.7S in gray. (C) Cumulative inactivation time course plotted as the fraction of the current left after each consecutive pulse ($I_{nth\ pulse}/I_{1st\ pulse}$ vs. pulse number). Smooth lines correspond to monoexponential fits (mKv1.7L in black, $n = 15$; and mKv1.7S in gray, $n = 12$). (D and E) Effect of different potassium concentrations over cumulative inactivation of mKv1.7L and mKv1.7S, respectively. Data are given as average values of four oocytes per $K^+$ concentration ($K^+_o$ in mM: ○, 2.5; △, 5; ■, 20; ▲, 50; ◆, 117.5).

channels; no p/n protocol was implemented for this type of experiment (Fig. 4, A and B). Plots of normalized test pulse current vs. pulse number were accurately fit with a monoexponential decay function. At 2.5 mM $[K^+]_o$, mKv1.7S showed slower cumulative inactivation kinetics than mKv1.7L (mKv1.7S $\tau_{CI}$, 8.14 ± 0.3 s; mKv1.7L $\tau_{CI}$, 22.5 ± 4.4 s, P = 0.0042; Fig. 4 C). The cumulative inactivation in both channel types was, to some extent, sensitive to extreme concentrations of $K^+$, however, mKv1.7L showed a graded and progressive response with increasing concentrations of potassium, whereas the cumulative inactivation of mKv1.7S did not (Fig. 4, D and E).

Taken together, these data indicate that translation of the channel at the second AUG codon and (as a consequence) the absence of the N-terminal fragment on the shorter form mKv1.7S has a critical effect by generating channels more resistant to inactivation at physiologically relevant potentials.

### Redox Modulation of mKv1.7 Channels

A striking effect was observed during patch clamp experiments, not only was the inactivation time constant of mKv1.7L-mediated currents ∼2.5 times smaller than the one of Kv1.7S in the on-cell configuration (mKv1.7L$\tau_{Inac}$= 26 ± 4 ms vs. mKv1.7S$\tau_{Inac}$= 66 ± 3 ms at +40 mV), but upon patch excision, mKv1.7L channels inactivated even faster (Fig. 5 A). For instance, Kv1.7L currents from inside-out patches decayed with an average $\tau_{Inac}$ of 11 ± 4 ms at a test potential of +40 mV, which is less than half the on-cell $\tau_{Inac}$ at the same potential. Although currents from mKv1.7S inside-out patches appeared slightly faster than the currents from on-cell measurements (Fig. 5 C), no significant difference could be detected (at +40 mV, mKv1.7S$\tau_{Inac}$ on cell = 71 ± 8 ms, mKv1.7S$\tau_{Inac}$ inside out = 66 ± 3 ms). Rundown of the currents from both channels was accelerated upon patch excision till complete current disappearance within a few minutes.

The finding that the inactivation of mKv1.7L currents varied in different experiments, and the observation that currents were faster in inside-out patches prompted us to examine the hypothesis that an intracellular "modulator" was washed away during patch excision. Other ion channels have proven to be sensitive to the oxidative state of the medium. Inside-out patches expose the cytoplasmic side of the plasma membrane to the environmental $O_2$ and $CO_2$ concentration (in equilibrium with the bath solution); in contrast, on-cell recordings are made under intracellular physiologically controlled redox conditions. As an alternative to circumvent the fast rundown of inside-out patches, we decided to investigate

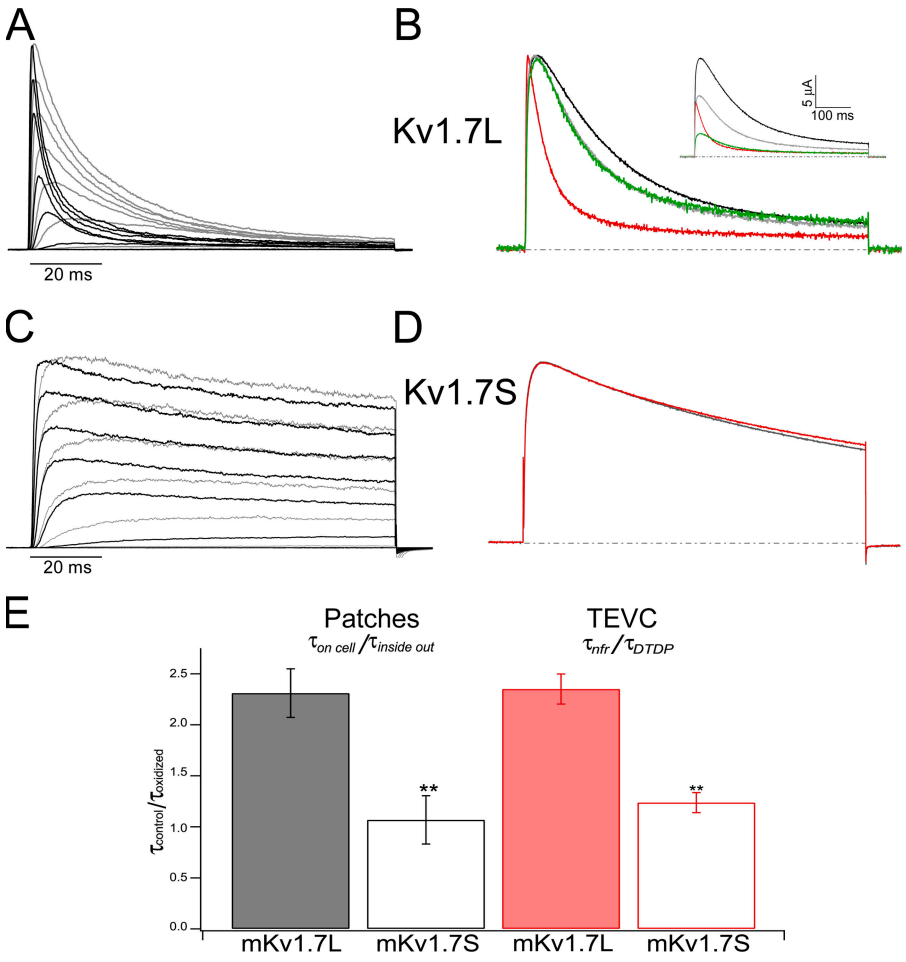


**Figure 5.** Redox sensitivity of mKv1.7. (A) Superimposed on-cell and inside-out patch clamp records from the same patch containing mKv1.7L channels. Gray corresponds to recordings in the on-cell configuration; black represents the currents under inside-out condition. Test pulses between −60 and +80 mV in 20-mV steps; $V_h = -100$ mV. (B) Normalized TEVC current traces from mKv1.7L exposed to different redox conditions (black corresponds to NFR; green, DTT; red, DTDP; and gray is washout with NFR). The inset presents the nonnormalized experiment. The dashed lines correspond to 0 current level. (C) mKv1.7S from a patch experiment (colors as in A). (D) mKv1.7S TEVC experiment (colors as in B). (E) Relative change in the inactivation time constant upon oxidation of Kv1.7L (solid bars, $n = 6$) and Kv1.7S (empty bars, $n = 4$) channels. Time constants obtained from monoexponential fits to the current decay upon +40-mV pulses under control conditions ($\tau_{control}$) divided by inactivation time constant under oxidizing conditions ($\tau_{oxidized}$, $\tau_{inside\ out}$, $\tau_{DTDP}$).

the influence of membrane-permeable reducing (dithiotreithol [DTT]) and oxidizing (dithiodipyridine [DTDP]) agents on Kv1.7 currents during TEVC experiments. Special care was taken in using oocytes with similar current kinetics under control conditions for each channel type in order to minimize potential variations in inactivation kinetics of Kv1.7 currents due to intrinsic variations of the redox state of individual oocytes. Exposure of oocytes expressing Kv1.7L to 200 µM DTDP decreased the peak current amplitude and speeded up inactivation about twofold (control $\tau_{Inac} = 218 \pm 3$ ms vs. DTDP $\tau_{Inac} = 94 \pm 4$ ms, at +40 mV). In Fig. 5 B, current traces were scaled to peak amplitude to demonstrate the acceleration of inactivation elicited by oxidation with DTDP on mKv1.7L currents. Washing with a reducing agent (DTT) resulted in partial reversal of the inactivation but no recovery in control peak amplitude; further wash with NFR completely rescued the control inactivation kinetics. Addition of the physiologically relevant oxidizing compound $H_2O_2$ to the extracellular bath had the same effect as DTDP, while a 2 mM $ZnCl_2$-supplemented NFR led to rapid recovery of slower inactivation kinetics during TEVC experiments (unpublished data). Nevertheless, complete reversal of DTT and/or DTDP effects was difficult to achieve since both chemicals traverse the membranes and can be trapped in different compartments in the oocyte, making the washout more difficult. Experiments with mKv1.7S and DTDP under the same conditions resulted in only a mild decrease of the current amplitude, without a significant change in kinetics (Fig. 5 D). Inactivation time constants before and after the exposure to oxidizing conditions during patch and TEVC experiments were compared at all potentials tested. In Fig. 5 E, the $\tau_{Inac}$ from currents recorded at +40 mV from mKv1.7L channels showed significant change (greater than twofold) when exposed to oxidizing conditions ($P < 0.001$) in very good agreement with the data from patches and TEVC. In contrast, mKv1.7S currents were not affected by either patch excision or DTDP exposure. Thus, the presence of the 32 amino acids in the N terminus of mKv1.7L appears to be a key component in the redox sensitivity of mKv1.7 channel inactivation.

### N-terminal Determinants of Inactivation and Redox Modulation

To investigate which amino acids are important for the redox modulation of mKv1.7L channels, mutations

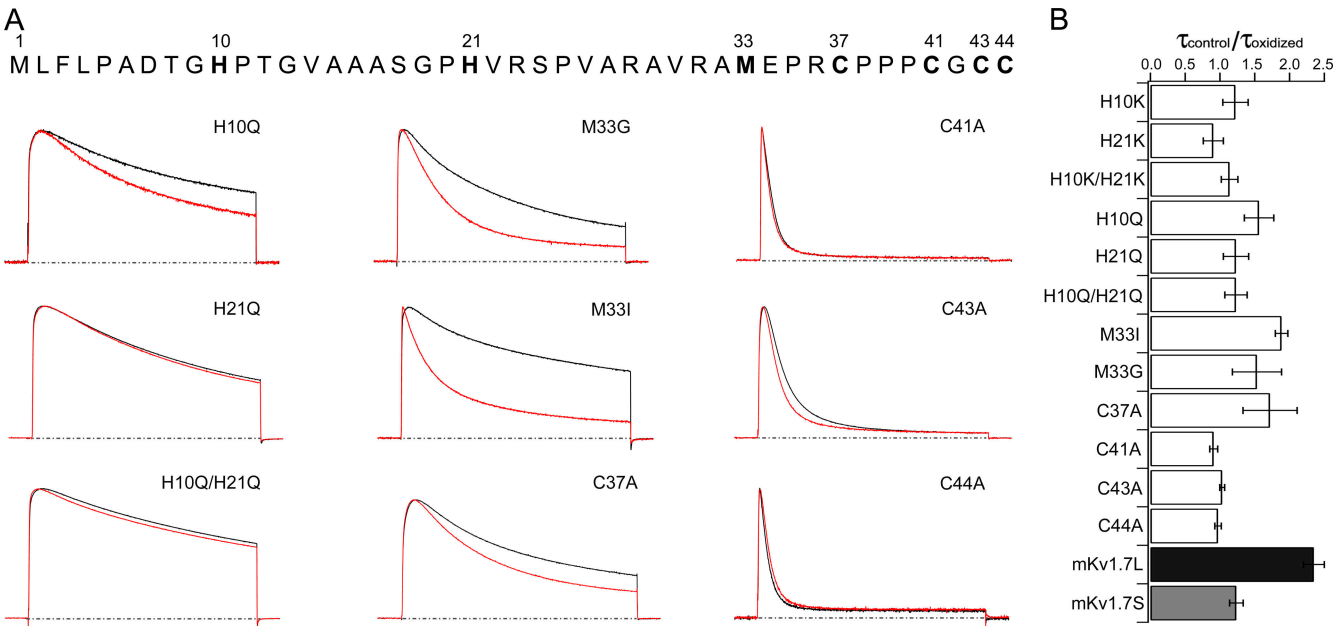


**Figure 6.** N-terminal determinants of mKv1.7 channels redox sensitivity. (A) Scaled and superimposed current traces of the different N terminus mutants (+40 mV, 500 ms, $V_h$ = −100 mV) of Kv1.7L. Black traces correspond to recordings under control conditions (NFR) and red traces are currents recorded in the presence of 300 μM DTDP. The dashed lines correspond to 0 current. Mutations are indicated in each panel. (B) Relative change in the inactivation time constant upon oxidation of mKv1.7 mutant channels. Time constants obtained from monoexponential fits to the current decay upon +40 mV pulses under control conditions ($\tau_{control}$) divided by inactivation time constant under DTDP oxidizing conditions ($\tau_{oxidized}$) (mean ± SEM; $n$ = 5–15).

involving amino acids sensitive to oxidation (histidines, methionines, and cysteines) in the N terminus were generated and expressed in *Xenopus* oocytes (Fig. 6 A). Table II summarizes the steady-state characteristics under control conditions of all mutants studied. Mutations of H10 and H21 to Lys or Gln resulted in significant leftward shifts in the half activation potential (Table II). The voltage dependence parameters of the H21K and H10K/H21K mutants were significantly shallower, while H10K, H10Q, and H10Q/H21Q were not altered, suggesting that the ionizable side chain of His21 might be relevant to the steady-state characteristics of the mKv1.7L channels (Table II; Fig. 6). When the methionine in position 33 of the Kv1.7L channel was mutated to Ile or Gly, the resulting $V_{1/2}$ was indistinguishable from that of mKv1.7S channels, although with inactivation kinetics resembling mKv1.7L channels. In addition, the $V_{1/2}$ of the C37A mutant was displaced to negative potentials, further suggesting interactions between the N-terminal region and the gating machinery of the channel. The steady-state activation parameters of the C41A, C43A, and C44A mutants were comparable to Kv1.7L channels.

The main changes induced by mutations at the N terminus of mKv1.7 channels were related to inactivation kinetics (Table II). Thus, H10K and H10Q mutants inactivate with a time constant approximately two times slower than the Kv1.7L channels. However, H21K and H10K/H21K inactivation kinetics were indistinguishable from mKv1.7L. Nevertheless, the H21Q mutation resulted in time constants approximately three times slower, similar to those observed for the mKv1.7S channels (Table II). Conversely, Ala substitutions of cysteines 41, 43, and 44, but not 37, resulted in significantly faster inactivation kinetics (Table II).

Finally, all the N-terminal mutants generated were subjected to 300 μM DTDP, and the inactivation time constants for control and DTDP exposure experiments were compared (Fig. 6). Fig. 6 A shows normalized current traces in response to +40 mV depolarizing pulses for the different mutant channels studied under control conditions and after oxidation. A loss of the oxidative effect on the inactivation kinetics was observed in the histidine mutant H21Q and the double mutant H10Q/H21Q; the single mutant (H10Q) retained oxidation sensitivity (Fig. 5 A). Methionine 33 does not seem to be an important target for oxidation (M33G and M33I were DTDP sensitive), although it might be involved in the inactivation process by steric hindrance since replacing Met33 with a bulkier residue (Ile) generated channels with slower kinetics than the M33G mutants. An Ala substitution at Cys37 resulted in faster inactivation kinetics under DTDP oxidizing conditions, showing that this residue may not be directly related to the phenomenon. Cysteines 41 and 44 when mutated to alanine inactivate both constitutively faster than mKv1.7L channels while they seem to have lost the sensitivity to oxidation. C43A mutants inactivate significantly

TABLE II

*Characteristics of the Currents Mediated by mKv1.7 Mutant Channels Expressed in Xenopus Oocytes Determined by TEVC Measurements*

| | Charge | $V_{1/2}$ | Slope | | $RT_{75}$ | | $\tau_{Inac}$ | |
|---|---|---|---|---|---|---|---|---|
| | | *mV* | *mV* | *n* | *ms* | *n* | *ms* | *n* |
| mKv1.7L | 7.45 | 4.4 ± 1.4 | 15.4 ± 0.5 | 20 | 4.4 ± 0.5 | 12 | 181.8 ± 15.4 | 15 |
| mKv1.7S | 5.12 | −4.3 ± 2.9 | 13.3 ± 0.6 | 15 | 7.5 ± 0.7 | 12 | 643.2 ± 80.1 | 13 |
| H10K | 8.28 | −5.3 ± 1.2[b] | 15.3 ± 1.0 | 7 | 7.2 ± 1.4[a] | 9 | 334.9 ± 40.1[c] | 7 |
| H21K | 8.28 | −10.1 ± 2.3[c] | 12.2 ± 0.7[b] | 7 | 11.0 ± 1.3[c] | 8 | 225.3 ± 9.0 | 8 |
| H10KH21K | 9.11 | −14.5 ± 2.6[c] | 11.0 ± 1.6[b] | 5 | 7.6 ± 0.8[b] | 5 | 230.4 ± 20.3 | 5 |
| H10Q | 7.28 | −5.1 ± 1.8[c] | 17.1 ± 1.1 | 7 | 3.4 ± 0.2 | 8 | 394.3 ± 65.8[c] | 7 |
| H21Q | 7.28 | −1.5 ± 1.7[a] | 17.5 ± 0.7 | 6 | 3.44 ± 0.3 | 6 | 516.6 ± 71.4[c] | 5 |
| H10QH21Q | 7.12 | −0.2 ± 1.2 | 17.8 ± 0.5 | 5 | 3.24 ± 0.2 | 6 | 632.5 ± 86.9[c] | 5 |
| M33I | 7.45 | −4.1 ± 1.2[b] | 17.2 ± 0.6 | 6 | 4.0 ± 0.5 | 8 | 244.2 ± 51.5 | 8 |
| M33G | 7.45 | −3.5 ± 2.1[a] | 14.9 ± 0.9 | 3 | 4.7 ± 0.8 | 5 | 127.9 ± 19.7 | 9 |
| C37A | 7.48 | −2.2 ± 1.4[b] | 16.6 ± 0.4 | 7 | 5.3 ± 0.7 | 9 | 232.7 ± 49.1 | 11 |
| C41A | 7.48 | −0.5 ± 1.2 | 17.0 ± 0.5 | 7 | 3.3 ± 0.3 | 7 | 76.0 ± 3.08[c] | 9 |
| C43A | 7.48 | −0.1 ± 1.4 | 15.4 ± 0.5 | 5 | 4.5 ± 0.4 | 5 | 89.2 ± 4.9[b] | 6 |
| C44A | 7.48 | −1.0 ± 1.7 | 17.7 ± 0.4 | 7 | 3.0 ± 0.1[a] | 8 | 65.4 ± 10.8[c] | 8 |
| Kv1.7S-H342G | 5.12 | −1.8 ± 3.1 | 16.5 ± 1.5 | 4 | 9.8 ± 1.0 | 4 | 737.6 ± 102.1 | 4 |
| Kv1.7S-C12A | 5.12 | −1.5 ± 1.0 | 14.7 ± 1.7 | 2 | 10.7 ± 1.8 | 2 | 1117.0 ± 38.4 | 2 |

Charge was determined at pH 7 for the N-terminal 182 aa or 150 aa in Kv1.7S. $RT_{75}$ and $\tau_{Inac}$ were determined at 40 mV.

[a]$P < 0.01$, compared to mKv1.7L.

[b]$P < 0.001$, compared to mKv1.7L.

[c]$P = 0.0001$, compared to mKv1.7L.

faster than mKv1.7L but still retain some sensitivity to oxidation (Fig. 5 A). Thus, amino acids H21, C41, C43, and C44 seem to be determinants of inactivation in mKv1.7 channels under control conditions, and are likely involved in the redox modulation of the channel. Equivalent mutations were made and expressed for mKv.17S channels without any effects in inactivation kinetics or redox sensitivity (C5A, C11A, and C12A; unpublished data).

## DISCUSSION

We have cloned, expressed, and characterized mouse heart muscle Kv1.7 channels. Since the cloned sequence predicted two putative initiation sites, we expressed and characterized the two resulting proteins. Our experiments prove that both AUGs are functional in heterologous systems, and expression at each AUG can potentially generate proteins with different characteristics: mKv1.7L channels that inactivate fast and are sensitive to redox modulation, and slow-inactivating, redox-insensitive mKv1.7S. Moreover we identified an arrangement of amino acids that are involved in the redox sensitivity of mKv1.7L channel that resembles metal coordination motifs observed in well-known redox-sensitive proteins.

The *Kcna7* cDNA clone amplified in this work is within a coding region flanked by well-defined stop codons and encodes mKv1.7 channels from the mouse heart and skeletal muscle (>90% identical to the mouse, human, and rat cDNA sequences from public databases). We amplified the 5′ cDNA fragment of the *Kcna7* clone with different primer sets in independent RT-PCR reactions obtaining exactly the same results; therefore, we are very confident in the correctness of our sequence. Furthermore, nucleotide alignment of the AF032099 cDNA clone (Kalman et al., 1998), AJ409348 mouse cDNA fragment (Kashuba et al., 2001), EST genomic fragment IMAGp998P111081Q3, mouse genomic sequence of the chromosome 7 (accession no. AC073711, nt 133775–137318 complementary strand), rat *Kcna7* putative gene located in chromosome 1 (accession no. NW_047558), and AY779767 (reported here) revealed a puzzling difference in the putative ORF of the mouse *Kcna7* gene. The first AUG codon generated the mKv1.7L protein of 489 aa in contrast to mKv1.7S (457 aa); the latter is equivalent to the proteins reported by Kashuba et al. (2001) and Bardien-Kruger et al. (2002). This first AUG is present in all the sequences aligned, but surprisingly it was not identified as a potential initiation of the translation point in any of the previous reports on *Kcna7*/mKv1.7 channels (Kalman et al. 1998, Kashuba et al. 2001; Bardien-Kruger et al., 2002). The presence of a weak Kozak consensus sequence flanking the first AUG, as well as the presence of a good one around the second AUG, seems not to impair the expression of large outward potassium currents with fast inactivation kinetics. Addition of an ideal Kozak around M1 or elimination of M33 (second initiation codon, mutants M33I and M33G) did not influence the expression of faster inactivating currents in comparison to mKv1.7S mutants. Furthermore, the functional expression of the M33 mutants confirms that translation of the

Kv1.7L channels must start at the first AUG (M1 in this work). Therefore, we have clear functional evidence that the translation of the mouse Kv1.7 channel results in a 489-aa protein characterized by fast inactivation kinetics. Other eukaryotic mRNAs have been described in which the 5′ proximal AUG codon occurs in a suboptimal context and, as a consequence, ribosomes initiate translation at both AUG codons, producing two proteins from one mRNA in a process recognized as "leaky scanning" (Kozak, 1999). Studies performed on Kv3.3 channels revealed that the inconsistencies in the inactivation rates obtained from heterologous expression in different cell types were related to a weak Kozak sequence around the first AUG start site, allowing translation to start at both AUGs, and consequently high variability in the inactivation kinetics of Kv3.3 channels was observed (Fernandez et al., 2003).

Exhaustive evidence from studies on the *Drosophila Shaker* channels, as well as other voltage-activated fast-inactivating ion channels, that the N-terminal domain is generally responsible for fast (N-type) inactivation has been published. The sequence of the mKv1.7L N-terminal region includes a hydrophobic and a positively charged region resembling characteristic motifs described for the inactivation peptides of *Shaker* channels (Murrell-Lagnado and Aldrich, 1993). Deletion of specific segments of the N terminus of mKv1.7 retarded inactivation in a manner comparable to reports for *Shaker*, *Aplysia* AKv1.1a, and Kv1.4 channels that are known to N-inactivate (MacKinnon et al., 1993; Furukawa, 1995; Lee et al., 1996).

Studies of the recovery from inactivation of *Shaker* B channels show that the slow time constant $\tau_1$ is $K^+_o$ sensitive while $\tau_2$ is not (Gomez-Lagunas and Armstrong, 1994), as is the case for mKv1.7 channels. The association between $\tau_1$ must be directly related to the N-type inactivation from which recovery is slow, while $\tau_2$ should be related to a second inactivation mechanism with slower kinetics but faster recovery. Labarca and MacKinnon proposed that high $K^+_o$ was able to displace the channels from an inactivated state to another from which they could be reopened (Labarca, P., and R. MacKinnon. 1992. *Biophys. J.* 61:A378). This is in agreement with the recovery from inactivation data presented in this study for mKv1.7; the recovery from inactivation of mKv1.7S channels was not affected by the presence of high $K^+_o$ while the recovery of the ionic currents of mKv1.7L was faster in isotonic potassium (Demo and Yellen, 1991). This supports the view that $K^+_o$ destabilizes the binding of the "ball peptide" to the inner cavity of the channel (Gomez-Lagunas and Armstrong, 1994).

mKv1.7L develops stronger cumulative inactivation under the same conditions than mKv1.7S. Recovery from inactivation of mKv1.7S was fast, while mKv1.7L recovery was speeded to the same level only in the presence of high $K^+$. Coherently, cumulative inactivation was modulated by extracellular potassium in the channels studied, particularly evident in the mKv1.7L channels where even small changes in the $[K^+]_o$ significantly slowed the cumulative inactivation rate. Baukrowitz and Yellen (1995) found that frequency-dependent cumulative inactivation of *Shaker* channels is sensitive to changes in $[K^+]_o$, especially in the physiological range, where much more inactivation was observed at low $[K^+]_o$, as we report for Kv1.7 channels. The authors conclude that such effect resulted from coupling of N- and C-type inactivation, where N-type inactivation could inhibit the $K^+$ efflux that prevents C-type inactivation, and simultaneously the binding of the N-particle extends the time that the activation gate would be open after repolarization, allowing C-type inactivation to occur for a prolonged period (Baukrowitz and Yellen, 1995). We do observe an antagonistic effect of $K^+$ from the extracellular media over the onset of the cumulative inactivation of Kv1.7 currents, indicating that indeed N- and C-type inactivation coexist in the channels studied. Furthermore, the graded effect observed between mKv1.7L and mKv1.7S is an indication of the extent at which each of the processes occur in the channels characterized in this work.

In the presence of high extracellular $K^+$, the recovery of mKv1.7L channels is significantly faster. The more pronounced effect of high extracellular $K^+$ on the cumulative inactivation time course of the mouse Kv1.7L channel must be linked to the sensitivity of the fast inactivation to the increase of the extracellular potassium concentration.

Various mutants of mKv1.7 in the N-terminal region (such as H10K and H21K) showed slower inactivation kinetics, suggesting that the ionizable nature of the histidines, particularly H21, might be important for faster inactivation. Furthermore, changes to I or G of M33 did not affect inactivation kinetics significantly, although the presence of the bulkier isoleucine generated slower kinetics than glycine. Therefore, it is likely that the effect observed might be due to steric hindrance. Additionally, C41A, C43A, and C44A presented significantly faster inactivation kinetics. Taken together, our results are in good agreement with the hypothesis that mKv1.7L channels inactivate predominantly due to an N-type–related mechanism, which is impaired in the mKv1.7S shorter form.

### Redox Modulation

Faster recovery from inactivation of *Shaker B* channels exposed to oxidizing agents was suggested to occur through enzymatic oxidation of the third methionine in the N-terminal inactivation domain of the channel (Ciorba et al., 1997, 1998). Kv1.4, a mammalian channel present in cardiac tissue, is sensitive to oxidation; in response to patch excision, oxidation of Cys13 results in

the loss of fast inactivation (Ruppersberg et al., 1991). Several other examples of $K^+$ currents modulated by oxidation have been documented in the literature (Vega-Saenz de Miera and Rudy, 1992; Duprat et al., 1995). The redox modulation of large-conductance $Ca^{+2}$-activated $K^+$ (BK) channels, which are key regulators of vascular smooth muscle tone (Nelson and Quayle, 1995; Toro et al., 1998), has been explained by sulfhydryl reduction/oxidation of thiol groups from Cys residues near the $Ca^{2+}$ bowl and from the RCK domain of the BK α-subunit (Tang et al., 2004; Zhang and Horrigan, 2005).

We have observed that (1) mKv1.7L channels inactivate significantly faster upon patch excision and in the presence of the oxidizing agents dithiodipyridine and $H_2O_2$, while removal of these compounds leads to reestablishment of slower inactivation kinetics; (2) oxidizing the Kv1.7L channel not only affects inactivation but also causes a decrease in current amplitude; and (3) faster inactivation is not observed for mKv1.7S currents upon patch excision nor speeding of the current decay in the presence of DTDP.

The analysis of the N terminus of mKv1.7L channels revealed several features suggesting its involvement in inactivation, with characteristics resembling the ball domain from *Shaker*. Our results show that amino acids H21, C41, C43, and C44 are determinants of the inactivation properties of mKv1.7 channels by a direct structural role, by conferring sensitivity to redox modulation, and/or being involved in the interaction with an "accessory" redox sensor. However, the marked effects observed upon mutation of a pattern resembling a metal coordination motif composed of histidines and cysteines ($HX_{20}CXCC$) (Beinert et al., 1997; Rulisek and Vondrasek, 1998; Auld, 2001) suggests a direct effect over the mKv1.7 channel α-subunit. Rundown of mKv1.7 currents in excised patches hindered more direct experiments with different metal ions and chelators. Nevertheless, in TEVC experiments, addition of zinc to oxidized mKv1.7L channels led to a rapid return to control kinetics, suggesting the potential identity of the metal ion coordinated in the N terminus of mKv1.7 (unpublished data).

It seems plausible that the oxidation-sensitive region (or an important component of it) of the mKv1.7 channel is in the N-terminal region of the protein and includes residues in the adjacency of the tetramerization domain (T1). A similar arrangement $HX_5CX_{20}CC$ has been shown to coordinate $Zn^{2+}$ in the T1, determining subunit recognition of *Shab*, *Shaw*, and *Shal* subfamily members, but has not been found to date in *Shaker* subfamily members (Bixby et al., 1999). The T1 domain of mKv1.7 seems to be essential for the functional expression of mKv1.7 channels, since mKv1.7L-Δ34-72, deletion mutant of mKv1.7 missing a part of the alleged T1 domain, resulted in nonfunctional channels (unpublished data). mKv1.7L, mKv1.7S, and single aa mutant channels expressed large outward currents, proving that the deletion (or point mutations) of the N terminus of Kv1.7 channels does not impair subunit recognition and/or stable tetramerization into functional channels.

The presence of a motif used by many other redox-sensitive proteins (for review see Auld, 2004) suggests that mKv1.7L channels could be using a similar mechanism to respond to oxidative insult.

Rearrangement of the mKv1.7 protein structure in response to oxidation would speed up the inactivation of the potassium conductance, reducing the net outward potassium current, therefore retarding the membrane repolarization. This implies a novel mechanism through which oxidants can inhibit Kv channel activity during enhanced oxidative stress. However, further structural and functional studies will be required to confirm this hypothesis.

Recently, the role of oxidative stress on the modulation of $K^+$ channels has been established as an important determinant of vasomotor function during pathological conditions (Liu and Gutterman, 2002). Oxidants such as endothelial $H_2O_2$ have been suggested to mediate hyperpolarization/relaxation of the heart vasculature (Shimokawa and Matoba, 2004). The faster inactivation kinetics of mKv1.7L channels is positively correlated to the presence of 32 amino acids in the N terminus that are absent in the mKv1.7S. Kv1.7 are active at potentials more positive than −20 mV and are redox sensitive; as a consequence, inhibition of Kv1.7-mediated currents might take part in the control of vasoconstriction by influencing the membrane potential.

Kv1.7 transcripts have been found in blood vessels such as mouse mesenteric artery (Fountain et al., 2001) and rat pulmonary artery smooth muscle cells (Davies and Kozlowski, 2001), where acute hypoxia decreases $I_{K+}$ by inhibiting Kv channel activity, resulting in membrane depolarization and attenuation of Kv channel expression (Platoshyn et al., 2001). Furthermore, Ördög et al. (2005) reports real-time quantitative RT-PCR data that supports high expression of *Kcna7* transcripts in human heart (atrium and ventricule). Therefore, the mRNA expression profile and redox modulation of the kinetics of Kv1.7 channels suggests that this protein may constitute a molecular component of the hypoxia-induced membrane depolarization response of heart muscle cells. Nevertheless further studies on the protein expression profile are necessary for the understanding of the physiological role of the Kv1.7 channel.

The authors thank Robert French, Martin Stocker, and Baldomero M. Olivera for their comments on the manuscript. We thank Michael Ferber, Mona Honemann, Michael Hollmann, Florentina Soto, Martin Stocker, Anna Boccaccio, Jelena Radulovic, Daniel Kerschensteiner, and Rafael Garcia for helpful discussions and technical assistance.

The research of the authors was supported by the Biofuture Prize of the German Ministry of Education and Research (Förderkennzeichen 0311859 to H. Terlau).

Olaf S. Andersen served as editor.

Submitted: 26 January 2006
Accepted: 8 June 2006

## REFERENCES

Armstrong, C.M., and F. Bezanilla. 1974. Charge movement associated with the opening and closing of the activation gates of the Na channels. *J. Gen. Physiol.* 63:533–552.

Armstrong, C.M., F. Bezanilla, and E. Rojas. 1973. Destruction of sodium conductance inactivation in squid axons perfused with pronase. *J. Gen. Physiol.* 62:375–391.

Auld, D.S. 2001. Zinc coordination sphere in biochemical zinc sites. *Biometals.* 14(3-4):271–313.

Bardien-Kruger, S., H. Wulff, Z. Arieff, P. Brink, K.G. Chandy, and V. Corfiel. 2002. Characterization of the human voltage-gated potassium channel gene, KCNA7, a candidate gene for inherited cardiac disorders, and its exclusion as cause of progressive familial heart block I (PFHBI). *Eur. J. Hum. Genet.* 10:36–43.

Baukrowitz, T., and G. Yellen. 1995. Modulation of K+ current by frequency and external [K+]: a tale of two inactivation mechanisms. *Neuron.* 15(4):951–960.

Beinert, H., R.H. Holm, and E. Munck. 1997. Iron-sulfur clusters: nature's modular, multipurpose structures. *Science.* 277:653–659.

Bezanilla, F., and C.M. Armstrong. 1977. Inactivation of the sodium channel: 1. Sodium current experiments. *J. Gen. Physiol.* 70:549–566.

Bixby, K.A., M.H. Nanao, N.V. Shen, A. Kreusch, H. Bellamy, P.J. Pfaffinger, and S. Choe. 1999. $Zn^{2+}$-binding and molecular determinants of tetramerization in voltage-gated $K^+$ channels. *Nat. Struct. Biol.* 6:38–43.

Brown, A.M. 2004. Cardiac potassium channels in health and disease. *Trends Cardiovasc. Med.* 7:118–124.

Ciorba, M.A., S.H. Heinemann, H. Weissbach, N. Brot, and T. Hoshi. 1997. Modulation of potassium channel function by methionine oxidation and reduction. *Proc. Natl. Acad. Sci. USA.* 94:9932–9937.

Ciorba, M.A., S.H. Heinemann, H. Weissbach, N. Brot, and T. Hoshi. 1999. Regulation of voltage-dependent $K^+$ channels by methionine oxidation: effect of nitric oxide and vitamin C. *FEBS Lett.* 442:48–52.

Davies, A.R., and R.Z. Kozlowski. 2001. Kv channel subunit expression in rat pulmonary arteries. *Lung.* 179:147–161.

Demo, S.D., and G. Yellen. 1991. The inactivation gate of the Shaker K+ channel behaves like an open-channel blocker. *Neuron.* 7(5):743–753.

Duprat, F., E. Guillemare, G. Romey, M. Fink, F. Lesage, M. Lazdunski, and E. Honore. 1995. Susceptibility of cloned K+ channels to reactive oxygen species. *Proc. Natl. Acad. Sci. USA.* 92:11796–11800.

Fernandez, F.R., E. Morales, A.J. Rashid, R.J. Dunn, and R.W. Turner. 2003. Inactivation of Kv3.3 potassium channels in heterologous expression systems. *J. Biol. Chem.* 278:40890–40898.

Fountain, S.J., A. Cheong, R. Flemming, L. Mair, A. Sivaprasadarao, and D.J. Beech. 2004. Functional up-regulation of KCNA gene family expression in murine mesenteric resistance artery smooth muscle. *J. Physiol.* 556:29–42.

Furukawa, Y. 1995. Accumulation of inactivation in a cloned transient $K^+$ channel (AKv1.1a) of *Aplysia*. *J. Neurophysiol.* 74:1248–1257.

Gomez-Lagunas, F., and C.M. Armstrong. 1994. The relation between ion permeation and recovery from inactivation of ShakerB K+ channels. *Biophys. J.* 67(5):1806–1815.

Hoshi, T., W.N. Zagotta, and R.W. Aldrich. 1990. Biophysical and molecular mechanism of Shaker potassium channel inactivation. *Science.* 250:533–538.

Kalman, K., A. Nguyen, J. Tseng-Crank, I.D. Dukes, G. Chandy, C.M. Hustad, N.G. Copeland, N.A. Jenkins, H. Mohrenweiser, B. Brandriff, et al. 1998. Genomic organization, chromosomal localization, tissue distribution, and biophysical characterization of a novel mammalian Shaker-related voltage-gated potassium channel, Kv1.7. *J. Biol. Chem.* 273:5851–5857.

Kashuba, V.I., S.M. Kvasha, A.I. Protopopov, R.Z. Gizatullin, A.V. Rynditch, C. Wahlestedt, W.W. Wasserman, and E.R. Zabarovsky. 2001. Initial isolation and analysis of the human Kv1.7 (KCNA7) gene, a member of the voltage-gated potassium channel gene family. *Gene.* 268:115–122.

Kozak, M. 1991. Structural features in eukaryotic mRNAs that modulate the initiation of translation. *J. Biol. Chem.* 266:19867–19870.

Kozak, M. 1999. Initiation of translation in prokaryotes and eukaryotes. *Gene.* 234(2):187–208.

Lee, T.E., L.H. Philipson, and D.J. Nelson. 1996. N-type inactivation in the mammalian Shaker $K^+$ channel Kv1.4. *J. Membr. Biol.* 151:225–235.

Li, M., Y.N. Jan, and L.Y. Jan. 1992. Specification of subunit assembly by the hydrophilic amino-terminal domain of the *Shaker* potassium channel. *Science.* 257:1225–1230.

Liman, E.R., J. Tytgat, and P. Hess. 1992. Subunit stoichiometry of a mammalian $K^+$ channel determined by construction of multimeric cDNAs. *Neuron.* 9:861–871.

Liu, Y., and D.D. Gutterman. 2002. Oxidative stress and potassium channel function. *Clin. Exp. Pharmacol. Physiol.* 4:305–311.

MacDonald, P.E., X.F. Ha, J. Wang, S.R. Smukler, A.M. Sun, H.Y. Gaisano, A.M. Salapatek, R.H. Backx, and M.B. Wheeler. 2001. Members of the Kv1 and Kv2 voltage-dependent K(+) channel families regulate insulin secretion. *Mol. Endocrinol.* 15:1423–1435.

MacKinnon, R., R.W. Aldrich, and A.W. Lee. 1993. Functional stoichiometry of *Shaker* potassium channel inactivation. *Science.* 262:757–759.

Murrell-Lagnado, R.D., and R.W. Aldrich. 1993. Interactions of amino terminal domains of *Shaker* K channels with a pore blocking site studied with synthetic peptides. *J. Gen. Physiol.* 102:949–975.

Nelson, M.T., and M.J. Quayle. 1995. Physiological roles and properties of potassium channels in arterial smooth muscle. *Am. J. Physiol.* 268:C799–C822.

Nerbonne, J.M. 2000. Molecular basis of functional voltage-gated $K^+$ channel diversity in the mammalian myocardium. *J. Physiol.* 525:285–298.

Ördög, B., E. Brutyo, L.G. Puskas, J.G. Papp, A. Varro, J. Szabad, and Z. Boldogkoi. 2005. Gene expression profiling of human cardiac potassium and sodium channels. *Int. J. Cardiol.* 10.1016/j.ijcard.2005.07.063

Platoshyn, O., Y. Yu, V.A. Golovina, S.S. McDaniel, S. Krick, L. Li, J.Y. Wang, L.J. Rubin, and J.X. Yuan. 2001. Chronic hypoxia decreases $K(_V)$ channel expression and function in pulmonary artery myocytes. *Am. J. Physiol. Lung Cell. Mol. Physiol.* 280(4):L801–L812.

Polder, H.R., J. Planck, M. Weskamp, M. Ferber, and H. Terlau. 2003. An electronic device that measures series resistance during TEVC recording in *Xenopus* oocytes. Poster at 29th Göttingen Neurobiology Conference 2003. *In* Proceedings of the 29th Göttingen Neurobiology Conference and the 5th Conference of the German Neuroscience Society. N. Elsner and H. Zimmermann, editors. Thieme, Stuttgart, abstract number 1084, 1069.

Pongs, O., T. Leicher, M. Berger, J. Roeper, R. Bahring, D. Wray, K.P. Giese, A.J. Silva, and J.F. Storm. 1999. Functional and molecular aspects of voltage-gated $K^+$ channel beta subunits. *Ann. NY Acad. Sci.* 868:344–355.

Roeper J., S. Sewing, Y. Zhang, T. Sommer, S.G. Wanner, and O. Pongs. 1998. NIP domain prevents N-type inactivation in voltage-gated potassium channels. *Nature.* 391:390–393.

Rulisek, L., and J. Vondrasek. 1998. Coordination geometries of selected transition metal ions ($Co^{2+}$, $Ni^{2+}$, $Cu^{2+}$, $Zn^{2+}$, $Cd^{2+}$, and $Hg^{2+}$) in metalloproteins. *J. Inorg. Biochem.* 71:115–127.

Ruppersberg, J.P., M. Stocker, O. Pongs, S.H. Heinemann, R. Frank, and M. Koenen. 1991. Regulation of fast inactivation of cloned mammalian IK(A) channels by cysteine oxidation. *Nature.* 352:711–714.

Sambrook, J., E.F. Fritsch, and T. Maniatis. 1989. Molecular Cloning. A Laboratory Manual. Second Edition. Cold Spring Harbor Laboratory Press, Cold Spring Harbor, NY.

Shen, N.V., and P.J. Pfaffinger. 1995. Molecular recognition and assembly sequences involved in the subfamily-specific assembly of voltage-gated K+ channel subunit proteins. *Neuron.* 14:625–633.

Shimokawa, H., and T. Matoba. 2004. Hydrogen peroxide as an endothelium-derived hyperpolarizing factor. *Pharmacol. Res.* 49:543–549.

Tang, X.D., M.L. Garcia, S.H. Heinemann, and T. Hoshi. 2004. Reactive oxygen species impair Slo1 BK channel function by altering cysteine-mediated calcium sensing. *Nat. Struct. Mol. Biol.* 11:171–178.

Toro, L., M. Wallner, P. Meera, and Y. Tanaka. 1998. Maxi-K(Ca), a unique member of the voltage-gated K channel superfamily. *News Physiol. Sci.* 13:112–117.

Vega-Saenz de Miera, E., and B. Rudy. 1992. Modulation of $K^+$ channels by hydrogen peroxide. *Biochem. Biophys. Res. Commun.* 186:1681–1687.

Zagotta, W.N., T. Hoshi, and R.W. Aldrich. 1990. Restoration of inactivation in mutants of Shaker potassium channels by a peptide derived from ShB. *Science.* 250:568–571.

Zhang, G., and F.T. Horrigan. 2005. Cysteine modification alters voltage- and $Ca^{2+}$-dependent gating of large conductance (BK) potassium channels. *J. Gen. Physiol.* 125:213–236.